ELSEVIER

Brain Research Bulletin 68 (2006) 285–292

BRAIN RESEARCH BULLETIN

www.elsevier.com/locate/brainresbull

Visual responses and afferent connections of the n. ventrolateralis thalami (VLT) in the pigeon (*Columba livia*)

Martin Schulte, Bettina Diekamp *, Martina Manns, Ariane Schwarz, Carlos Valencia-Alfonso, Janina A. Kirsch, Onur Güntürkün, Kristian Folta

Fakultät für Psychologie, Biopsychologie, Ruhr-Universität Bochum, D-44780 Bochum, Germany

Received 19 July 2005; accepted 30 August 2005
Available online 22 September 2005

Abstract

The nucleus ventrolateralis thalami (VLT) in pigeons receives direct retinal and forebrain projections and has reciprocal connections with the optic tectum. Although VLT is a component of the avian visual system, no study directly examined its connections or its cellular response characteristics. We, therefore, recorded from single units in the pigeon's VLT while visually stimulating the ipsi- and/or contralateral eye. In addition, tracing experiments were conducted to investigate its afferent connections. Electrophysiologically, we discovered three types of neurons, two of which were probably activated via a top-down telencephalotectal system (latencies > 100 ms). Type I neurons responded to uni- and bilateral and type II neurons exclusively to bilateral stimulation. Type III neurons were probably activated by retinal or retinotectal input (latencies < 27 ms) and responded to contra- and bilateral stimulation. Retrograde tracer injections into the VLT revealed an ipsilateral forebrain input from the visual Wulst, from subregions of the arcopallium, and bilateral afferents from the optic tectum. Most intriguing was the direct connection between the VLTs of both hemispheres. We suggest that the avian VLT is part of a system that integrates visuomotor processes which are controlled by both forebrain hemispheres and that VLT contributes to descending tectomotor mechanisms.

Keywords: Avian; Birds; Visual system

1. Introduction

Visual information in birds is processed in parallel by the thalamo- and the tectofugal pathways which are equivalent to the mammalian geniculo-cortical and extrageniculo-cortical visual systems, respectively [41]. The thalamofugal pathway transfers retinal input to the contralateral thalamic nucleus geniculatus lateralis, pars dorsalis (GLd), which projects bilaterally to the visual Wulst of the forebrain [6]. The tectofugal pathway consists of retinal projections to the contralateral optic tectum (OT), from which fibers lead bilaterally to the nucleus rotundus (Rt), which then exclusively projects to the ipsilateral entopallium in the forebrain ([11,17,26]; terminology according to [33]). Due to the virtually complete decussation of the bird's optic nerves and the small amount of recrossings in the ascending pathways, each hemisphere receives information almost exclusively from the contralateral eye. Consequently, there is a strong need for interhemispheric integration of visual information from both eyes. Apart from the ascending systems, several further systems enable interhemispheric communication, like the tectotectal commissures, or the bilateral descending Wulst-tectum connections, which additionally serve as an important link between thalamo- and tectofugal systems [1,2,3,13,29]. The presence of bilateral connections of the pretectal nuclei [7,41,42] or the isthmic nucleus semilunaris [19] suggests modulatory visual nuclei to also play a critical role in interhemispheric communication.

The nucleus ventrolateralis thalami (VLT) is another good candidate for an interhemispheric integration of visual information. Although several studies refer to VLT as a distinct thalamic nucleus (Rendahl [35], who labeled it n. superficialis internus) [25,27,28,36,39], VLT has never been the focus of detailed investigations. As a side product of tracer injections, several studies have shown that VLT receives direct retinal projections [10,24,32,39,40], has bilateral and reciprocal connections

* Corresponding author. Present address: Department of Psychological and Brain Sciences, Johns Hopkins University, Baltimore, MD 21218, USA. Tel.: +1 410 516 0228/5148; fax: +1 410 516 6205/4478.
E-mail address: b.diekamp@jhu.edu (B. Diekamp).

0361-9230/$ – see front matter © 2005 Elsevier Inc. All rights reserved.
doi:10.1016/j.brainresbull.2005.08.019

with the optic tectum [4,21,22] and receives efferents from the visual Wulst [5,30,31,43]. However, no study has attempted to study directly the connections of VLT by tracer injections. Similarly, response characteristics of VLT neurons have never been studied. In this study, we combined for the first time electrophysiological recordings and anatomical tracing techniques to characterize this 'uncharted' thalamic structure and provide a first basis for speculations about its functional role in avian visual information processing.

2. Materials and methods

2.1. Animals

The original research reported herein was performed according to the principles regarding the care and use of animals for experimental procedures adopted by the National Institutes of Health Guide, the Society for Neuroscience and the specifications of the German Animal Welfare Law for the prevention of cruelty to animals. The successful cases totaled seven adult naïve homing pigeons (*Columba livia*) of both sexes which were obtained from local breeders in Germany.

2.2. Procedure

2.2.1. Surgery, stimulation and recording

Electrophysiological recordings were performed in five pigeons. The animals were anesthetized with 25% urethane (1 ml/100 g, i.m.) and the brain was exposed above the target area. Electrodes were placed stereotaxically at a 90° angle (45° upwards relative to the pigeon atlas by Karten and Hodos [25]). The eyelids of both eyes were kept open with adhesive tape. Light-conducting oculars connected to a halogen light (luminance: 40 or 900 cd/m^2; background illumination: 5 lux) were placed in front of the eyes to present diffuse light stimuli to the whole visual field of each retina. They were arranged in an angle of 60° to the left and right from midline, corresponding to the optical axis. This guaranteed that light was transferred only to the appropriate eye. Mechanical shutters (rise/fall times 27 ms each) were used to control stimulus presentation (500 ms) to the left and/or right eye. The interstimulus-interval was 5 s. Data acquisition started 100 ms before stimulus onset, which was defined as the point in time when luminance had reached 10% of its maximum. Four different stimulus conditions were tested: monocular stimulation of the eye either ipsilateral or contralateral to the recording site, simultaneous stimulation of both eyes and a control condition without stimulation.

Extracellular single cell responses were recorded from the right and the left VLT with single platinum–iridium electrodes (0.5–1 MΩ) or a multielectrode array (Thomas Recording, Giessen, Germany) of seven concentrically arranged electrodes (0.2–2.1 MΩ) using standard techniques described in detail in Folta et al. [13]. Neuronal signals were amplified ($\times 10^4$) and filtered (0.3–10 kHz). Single units responding to visual stimulation were recorded at depths between 9000 and 11,000 μm, stored and further isolated off-line by means of spike sorting and cluster cutting (EWB, DataWave Technologies; Spike 2, CED, Cambridge).

For histological verification of the recording sites, electrolytic lesions were placed at the end of each experiment at defined coordinates within the recording area with a steel electrode for the Prussian blue reaction ([14,15]; see methods in [13]). Animals were then perfused transcardially with saline and a 4% paraformaldehyde plus 15% potassium ferricyanide solution in 0.12 M phosphate buffer, pH 7.4. Brains were sagittally cut at 40 μm and brain sections were processed with standard histological methods.

Electrode tracts were verified in Nissl stained parasagittal brain sections and by lesion marks from the Prussian blue reaction. We carefully checked that extensions of electrode tracks passed directly through VLT and not through adjacent visual areas, such as n. rotundus, which is located more posterior to VLT. The coordinates of all electrode penetrations and the depths of recording sites relative to the lesions marks allowed a good reconstruction of the location of all recorded neurons.

2.2.2. Data analysis

Peri stimulus time histograms (PSTHs, 5 ms bin width) were calculated for each experimental condition. Neuronal activity was analyzed over a 250 ms interval after stimulus onset, since all isolated neurons responded exclusively to stimulus onset. Stimulus onset was defined as the point in time after opening of the shutter when luminance had reached 10% of its maximum. Spontaneous activity during control conditions was calculated within a 250 ms time interval. *T*-tests for dependent samples confirmed the statistical significance of responses to visual stimulation versus spontaneous activity for each isolated single unit. Normalized PSTHs were calculated for each unit by dividing the number of spikes in each bin by the maximal number of spikes, resulting in bin values between 0 and 1. Response latency was calculated as the lower time limit of two consecutive bins with normalized activity values of at least 0.33. Response offset was defined as the upper time limit of the first bin followed by two bins below the threshold of 0.33. Response duration was calculated as the time between response on- and offset. Peak activity strength was calculated by averaging the discharge rate (spikes/s) during the interval of significant spiking activity, as defined by response latency and duration. Finally, Friedman ANOVAs and Wilcoxon matched pairs tests were used to test for differences in response latency, peak activity strength and response duration within classes of neurons between different stimulus conditions. Mann–Whitney *U* tests were performed to test for differences between different classes of neurons.

2.2.3. Tracing experiments

Tracing experiments were performed in two adult pigeons with cholera-atoxin subunit B (CtB; Sigma). Pigeons were anesthetized with equithesin (0.31 ml/100 g, i.m.) and a glass micropipette (outer tip diameter 20 μm) was stereotaxically placed into the left VLT (A7.0, L3.0, D5.0, coordinates based on Karten and Hodos [25]). Thirty to forty nanoliters of CtB solution (1%, w/v in distilled water) were pressure-injected (Nanoliterinjector, WPI) over a 20 min period. After 2 days of survival, pigeons were anesthetized and perfused as described above (without the supplement of potassium ferricyanide). Brains were cut in frontal plane at 40 μm and collected in phosphate buffer containing 0.1% sodium azide (w/v). Brain slices were reacted free-floating with the immuno-ABC-technique as outlined in detail by Hellmann and Güntürkün [18]. The tracer injection sites and resulting retrograde CtB-labeling were reconstructed using a Leica DMR microscope. Digital images were processed with the AXIOVISION 3.0 software (Zeiss, FRG). Contrast and brightness were adjusted with Photoshop software (Adobe, Mountain View, CA).

3. Results

3.1. Identification of recording positions

We isolated 18 neurons within VLT, which showed a significant visual response in at least one of the three stimulation conditions as compared to spontaneous cell activity (*T*-tests). The location of 'Prussian blue' marks and the careful reconstruction of the electrode tracks confirmed that all recording sites were located within VLT and not in surrounding nuclei or fiber structures (Fig. 1).

3.2. Analysis of recorded cell responses

We classified all recorded neurons into three distinct groups based on their response characteristics (Table 1). Type I neurons ($n = 5$) were characterized by a short burst (10–30 ms duration) after contra-, ipsi- and bilateral stimulation of the eyes (Fig. 2). Response latencies differed significantly between the three stimulation conditions (Friedman ANOVA, $\chi^2 = 8.44$, $n = 5$, d.f. = 2, $p < 0.015$). Latencies were similar for contra- and ipsilateral visual input (averaging at 115.0 and 116.0 ms, respectively, Table 1), but were significantly longer for binocular stimulation

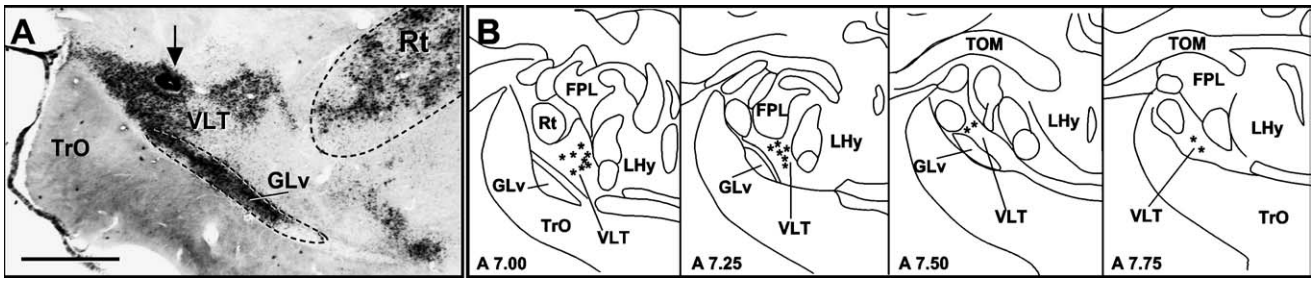

Fig. 1. (A) Electrode mark (arrow) within the n. ventrolateralis thalami (VLT) after passing a current and processing of the tissue for Prussian blue histochemistry. The parasagittal Nissl-stained section corresponds to a lateral plane at about L 2.50 (Karten and Hodos [25]). Rostral and dorsal are left- and upward, respectively. Scale bar = 1.0 mm. (B) Histologically verified recording sites in VLT shown in schematic frontal planes between A 7.00 and A 7.75 (Karten and Hodos [25]). VLT is situated in the rostroventral diencephalon and is surrounded by the n. geniculatus lateralis, pars ventralis (GLv) and the n. rotundus (Rt). Further abbreviations: lateral forebrain bundle (FPL), regio lateralis hypothalami (LHy), tractus occipitomesencephalicus (TOM) and tractus opticus (TrO). Lateral and dorsal are left- and upward, respectively.

(145.0 ms; Wilcoxon matched pairs tests, $Z = 2.023$, $p < 0.043$ for both bino-monocular comparisons). Response durations varied also significantly depending on the stimulation condition (Friedman ANOVA, $\chi^2 = 8.44$, $n = 5$, d.f. = 2, $p < 0.015$). They were comparable in response to contra- and ipsilateral visual input ($Z = 0.535$, $p < 0.593$) with shorter responses to binocularly presented stimuli (mean: 13 ms) compared to monocular visual stimulation (contralateral: 22 ms; ipsilateral: 23 ms; $Z = 2.023$, $p < 0.043$ for both tests). Peak activity strength differed significantly between the three stimulation conditions (Friedman ANOVA, $\chi^2 = 7.6$, $n = 5$, d.f. = 2, $p < 0.022$). It was similar after ipsi- and contralateral stimulation (90.8 and 84.0 spikes/s, respectively) but showed a significant difference to binocularly presented stimuli (132.7 spikes/s) compared to each monocular stimulation condition ($Z = 2.023$; $p < 0.043$ for both tests).

Type II neurons ($n = 5$) only responded to binocularly presented visual stimuli (Fig. 2). These neurons had a mean response latency of 82.0 ms, a mean response duration of 63.0 ms

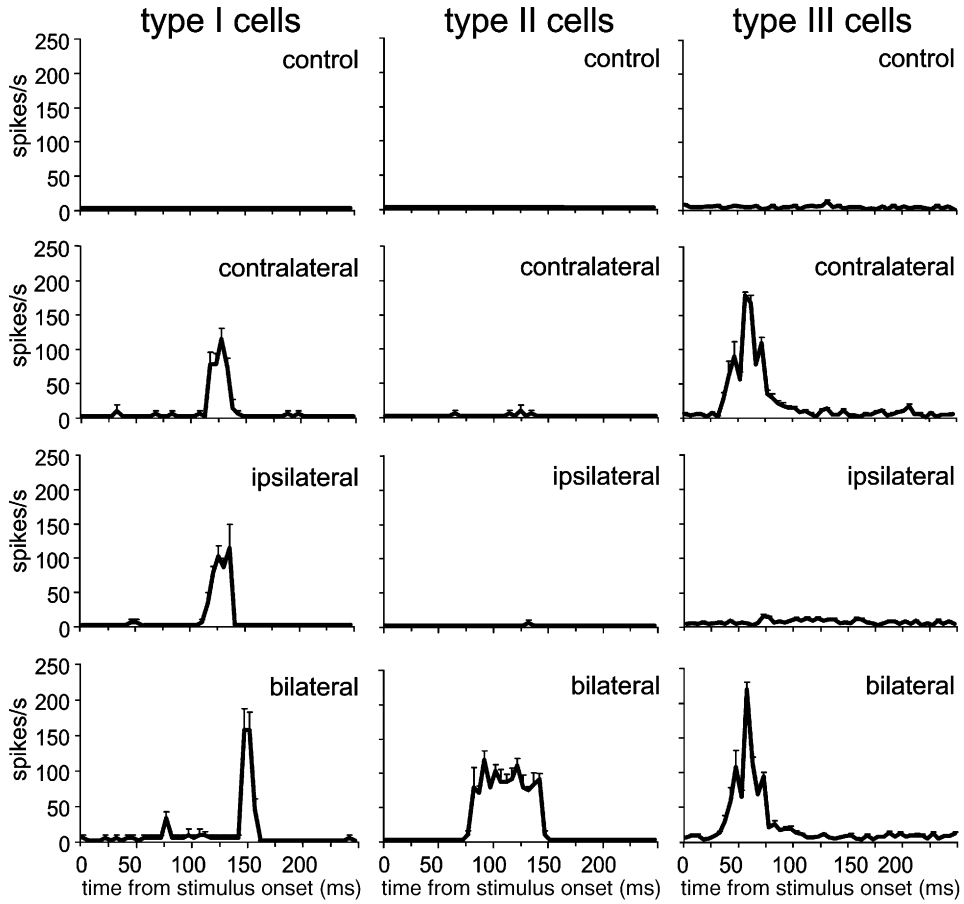

Fig. 2. Averaged spike activity of type I, type II and type III cells recorded in the ventrolateral thalamus in the control condition and in response to contralateral, ipsilateral and binocular stimulation. Solid thick lines represent the mean spike activity and whiskers the standard errors for each bin. Bin width = 5 ms.

Table 1
Response characteristics of the three classes of neurons

Response characteristics	Cell type		
	Type I ($n = 5$)	Type II ($n = 5$)	Type III ($n = 8$)
Spontaneous activity			
Rate (spikes/s)	0	0	2.8 (±1.56)
Contralateral visual stimulation			
Latency (ms)	115.0 (±0.0)	–	26.7 (±6.4)
Duration (ms)	22.0 (±4.5)	–	23.1 (±7.0)
Peak activity strength (spikes/s)	84.0 (±24.8)	1.2 (±2.0)	149.5 (±65.5)
Ipsilateral visual stimulation			
Latency (ms)	116.0 (±4.2)	–	–
Duration (ms)	23.0 (±2.7)	–	–
Peak activity strength (spikes/s)	90.8 (±33.4)	0.3 (±0.7)	5.5 (±2.7)
Binocular stimulation			
Latency (ms)	145.0 (±0.0)	82.0 (±2.7)	25.7 (±7.4)
Duration (ms)	13.0 (±2.7)	63.0 (±2.7)	25.0 (±9.6)
Peak activity strength (spikes/s)	132.7 (±48.8)	87.8 (±15.6)	135.8 (±58.2)

Values indicate mean (±standard deviation).

and a peak activity strength of 87.8 spikes/s in response to a binocular stimulus.

Type III neurons ($n = 8$) responded to contralateral and to binocular stimulation (Fig. 2). The response latencies were 26.7 ms for stimulation of the contralateral and 25.7 ms for stimulation of both eyes. The duration of the responses were 23.1 (contralateral) and 25.0 (bilateral); peak activity strength was 149.5 and 135.8 spikes/s, contra- and bilateral, respectively. Wilcoxon tests did not show differences in latencies, duration and peak activity strength between the contra- and bilateral stimulation ($Z > 1.26$, n.s. for all tests).

Comparisons between these three types of neurons revealed that responses of type II cells to a bilateral visual stimulus occurred significantly earlier and lasted significantly longer than those of type I cells (Mann–Whitney U tests; $Z = 2.61$, $p < 0.008$, for both tests), but there was no significant difference in peak activity strength ($Z = 1.57$, $p < 0.151$). Considering that latencies of type I cells were shortest in response to an ipsilateral visual stimulus, we compared the latencies of type II cells under binocular visual stimulus conditions to the shortest latencies of type I cells, i.e. under ipsilateral stimulation conditions. Even in this case, latencies of type II cells were significantly shorter than the shortest latencies of type I cells ($Z = 2.61$, $p < 0.008$). Also, response durations to bilateral stimulation were significantly longer in type II cells as compared to the longest response durations of type I cells, which occurred under ipsilateral stimulation conditions ($Z = 2.61$, $p < 0.008$). However, there was no significant difference in peak activity strength when comparing the bilateral responses of type II cells with ipsilateral ($Z = 0.63$, n.s.) or contralateral responses ($Z = 0.0$, n.s.) of type I cells.

Comparing the responses of type III and type I neurons for contra- and bilateral stimulation Mann–Whitney U tests showed differences in latencies (contralateral: $Z = 3.06$, $p < 0.05$; bilateral: $Z = 3.08$, $p < 0.05$), in duration only for binocular stimulation ($Z = 2.79$, $p < 0.05$) and in peak activity strength only for contralateral stimulation ($Z = 2.35$, $p < 0.05$). In the bilateral stimulation condition type III and type I neurons differed significantly in latency ($Z = 3.01$, $p < 0.05$), duration ($Z = 2.99$, $p < 0.05$) and in peak activity strength ($Z = 2.34$, $p < 0.05$). These analyses show that type III neurons responded significantly earlier than type I and type II neurons. Furthermore, the duration of type III neuron responses was shorter and the peak activity strength was higher than type II neurons (bilateral stimulation). The response duration of type I neurons was shorter for bilateral stimulation and the peak activity strength was lower for contralateral stimulation compared to type III neurons.

3.3. Analysis of CtB injections

Two adult pigeons received injections of the neuronal tracer CtB into the left VLT. In both cases, CtB injections resulted in a complex retrograde labeling pattern within the left diencephalon (Table 2). The reconstruction of the injection sites revealed that tracer spread was almost completely restricted to the area of the VLT with a small spread into the lateral forebrain bundle but did not include Rt, n. geniculatus lateralis, pars ventralis (GLv), or optic tract (Fig. 3A). We observed labeled cells in several surrounding structures of VLT and in subnuclei of the pigeon's GLd. Since it cannot be excluded that these cell labelings resulted from tracer spread into surrounding structures or penetration of the injection cannula into the fasciculus prosencephali lateralis (FPL) in the case of the GLd, they were not listed in Table 2. Apart from that, we identified labeled cells in various areas of the pigeon's brain that very likely do not result from tracer spread, e.g. in various layers of the optic tectum (OT), in

Table 2
Areas with labeled neurons and fiber staining after CtB injections into the left nucleus ventrolateralis thalami (VLT)

Structure	Cases #1/#2
Telencephalic nuclei	
Hyperpallium apicale (HA)	x
Arcopallium dorsale (AD)	xx
Arcopallium intermedium (AI)	x*
Arcopallium mediale (AM)	x
Ventrolateral thalamic nuclei	
n. ventrolateralis thalami (VLT)	x*
Hypothalamus	
regio lateralis hypothalami (LHy)	x
Pretectal mesencephalic nuclei	
n. isthmi pars semilunaris (SLu)	xx
Optic tectum	
Layer 4	x
Layer 6	x
Layers 8–9	x
Layers 10–11	xx
Layer 12	x
Layer 13	xx*
Layer 14	x

Note: The labeling patterns were identical in distribution and density for both histological cases. Abbreviations are according to the pigeon atlas by Karten and Hodos [25] and the new nomenclature for avian brain structures by Reiner et al. [33]. x: moderate labeling, xx: denser labeling, *: contralateral labeling.

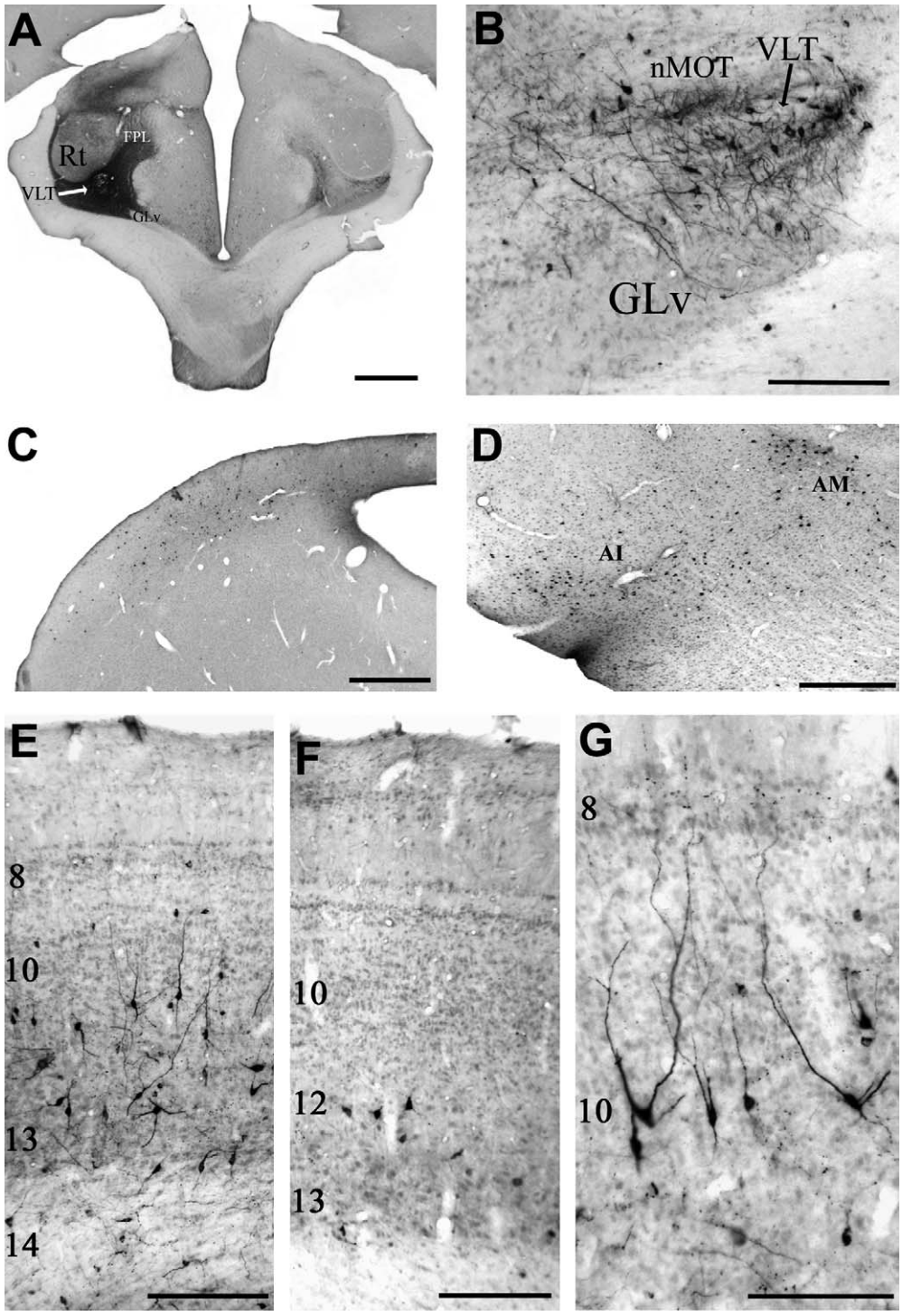

Fig. 3. CtB injections into the left n. ventrolateralis thalami VLT (A) resulted in retrogradely labeled neurons within the contralateral VLT (B), the ipsilateral visual Wulst (C) and arcopallium (D) as well as ipsilaterally (E) and contralaterally (F) labeled tectal neurons; a subpopulation of ipsilateral layer 10 cells ascended dendrites up to layer 5 (G). *Abbreviations*: arcopallium intermedium (AI), arcopallium mediale (AM), fasciculus prosencephali lateralis (FPL), n. geniculatus lateralis, pars ventralis (GLv), n. tractus optici marginalis (nMOT), n. rotundus (Rt). Scale bars = 1000 μm in (A and C), 500 μm in (D), 200 μm in (B, E and F).

the hyperpallium apicale (HA), various parts of the arcopallium, the contralateral VLT, the regio lateralis hypothalami (LHy) and the n. isthmi pars semilunaris (SLu; Figs. 3 and 4).

Overall, the labeling pattern was consistent and unambiguous for the two cases (Table 2). Retrograde CtB transport resulted in bilateral labeling of tectal neurons predominantly located within the ventrolateral tectum (Fig. 3E–G). Two cellular populations could be distinguished by their laminar distribution and their dendritic arborization pattern. Cells within the superficial layers 4–11 were confined to the lateral portion of the ipsilateral tectum (Fig. 3E). Layers 10 and 11 contained mainly small and medium sized radial cells. The apical dendrites of

these cells ascended to superficial tectal layers up to layer 5, but mostly terminated in layer 7, where they showed massive dendritic arborizations (Fig. 3G). Only few small labeled cells were observed in retinorecipient tectal layers 4 and 6. Labeled cells within the deeper layers 13–15 could be predominantly detected within the ventrolateral portion of the tectum. While cells located contralaterally to the injection side were confined to the superficial part of the ventral layer 13 (Fig. 3F), ipsilaterally projecting cells were located within laminae 13–15 (Fig. 3E). These cells were mainly multipolar, characterized by different size and shape and were mostly concentrated at the superficial border to layer 12. Dendritic arborizations could not be detected higher than up to layer 12. Thus, this deep population resembles cells of the descending tectal output [20]. Moreover, massive labeling of multipolar cells was observed mainly in the ventral part of the ipsilateral nucleus isthmi, pars semilunaris (SLu, A 1.75–A 2.25; Fig. 4).

In addition, we identified a telencephalic labeling in the ipsilateral visual Wulst (Fig. 3C) and the ipsilateral arcopallium (Fig. 3D). CtB-labeled cells in HA were widely distributed (A 7.5–A 9.5) and extended laterally up to the area temporo-parieto-occipitalis (TPO). A strikingly dense cluster of ipsilaterally labeled cells were also obtained in the outermost medial parts of the arcopallium dorsale (AD). According to the atlas of Karten and Hodos [25], these cells were distributed between A 6.25 and A 7.25. Furthermore, we observed clusters of labeled cells in the dorsal and ventrolateral part of AI between A 6.25 and A 7.0. Only few cells were labeled in the arcopallium mediale (AM) and were concentrated mainly at A 6.5 (Fig. 3D).

CtB injections also revealed retrogradely labeled multipolar neurons within the contralateral VLT (A 7.0–A 7.5), indicating a direct interthalamic connection between the ventrolateral thalami of the left and the right half brain (Fig. 3A and B). The cells displayed dendrites reaching ventrally into GLv and dorsally into the nucleus marginalis tractus optici (nMOT) while the localization of the cell bodies was clearly separated from nMOT.

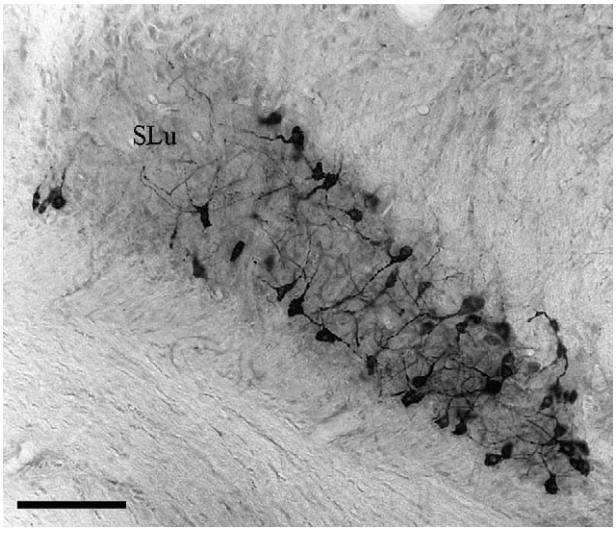

Fig. 4. CtB injections into the n. ventrolateralis thalami (VLT) labeled neurons within the ventral portion of the ipsilateral n. isthmi pars semilunaris (SLu). Scale bar = 100 μm.

4. Discussion

The present study provides the first evidence for both the existence of visually responsive units in the VLT along with anatomical results on the afferent connectivity of this uncharted territory of the avian diencephalon. Although our sample is small, it is important to emphasize the difficulty to inject into or record from such a tiny nucleus at the ventral base of the diencephalon. Our combined electrophysiological and anatomical data reveal that VLT could play a key role in the integration of visual information from both sides of the visual system (Fig. 5).

4.1. Response characteristics of VLT neurons

Our single unit recordings clearly show that VLT units are visually responsive. Since VLT receives direct retinal [32] and tectal input [21], all reported type III cells with short latencies of about 26 ms probably reflect bottom-up processing via a direct retinal or an indirect retinotectal path. Type I and type II cells had considerably longer latencies of more than 80 ms and could

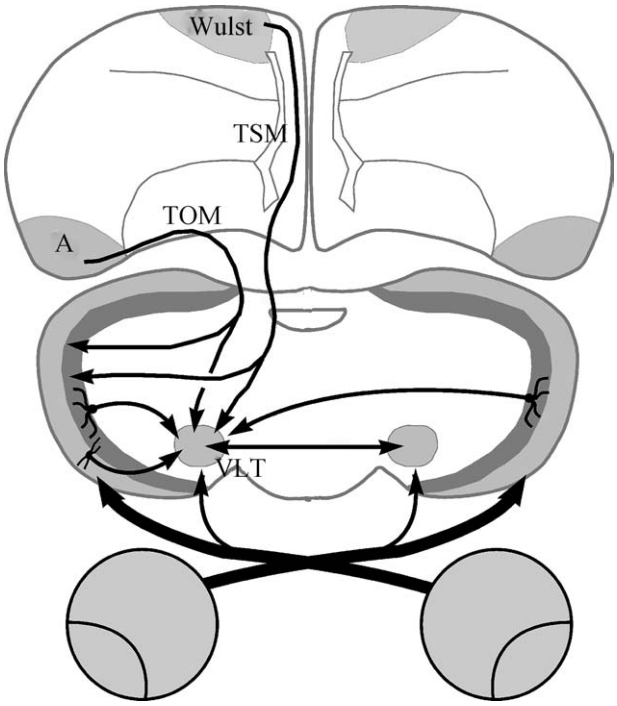

Fig. 5. Schematic diagram illustrating the connectivity of the n. ventrolateralis thalami (VLT). The depicted frontal section does not correspond to a real frontal plane. To avoid confusion, only a part of the connectivity of the VLT of one hemisphere is shown. Different tectal shadings correspond to the retinorecipient layers 2–7 (light grey) and intermediate as well as deep layers 8–15 (dark grey). Within the tectum two cardinal neurons are shown. The one within the retinorecipient layers has narrow dendritic fields and ipsilateral projections to VLT. The deep tectal neurons with wide dendritic endings have bilateral VLT-projections. *Abbreviations*: A (arcopallium), TOM (tractus occipitomesencephalicus), TSM (tractus septomesencephalicus).

reflect activity patterns of a top-down pathway. Indeed, Folta et al. [13] revealed rotundal cells with similarly long latencies that were selectively affected by an inactivation of the visual Wulst. Because the rotundus receives no direct projection from the visual Wulst but indirect ones via the tectum, the similarity of long response latencies in VLT and rotundus suggests that most of the late VLT responses might be attributable to a telencephalo-tecto-VLT transmission. The latency difference between unilateral and bilateral stimulation in type I cells might then be due to different intratectal mechanisms mediating either uniocular or binocular input. This assumption is strengthened by the observation that the higher peak activity strength after binocular than after monocular stimulation does not reflect a simple summation.

All recorded neurons were responsive to photic stimulation of both eyes. Type II cells even required simultaneous input from both eyes. The responses of type III neurons to bilateral stimulation did not differ from the responses to contralateral stimulation and therefore are most likely evoked only by the contralateral eye. Thus, at least the forebrain-mediated activation patterns of VLT seem to compute visual events within both visual fields.

4.2. Afferents of VLT

The forebrain afferents of VLT arose from the HA of the visual Wulst as well as from the arcopallial subfields AD, AI and AM. The Wulst projections were possibly mediated by the tractus septomesencephalicus (TSM) [31], while those from the arcopallium very likely ran through the tractus occipitomesencephalicus (TOM) [8] (Fig. 4). The visual Wulst is the primary telencephalic representation of the thalamofugal system [37]. The arcopallium receives visual input via both the entopallium [23] and a small projection from the Wulst [38]. Consequently, photic eye stimulations produce arcopallial responses with latencies of 40 ms [44]. Thus, forebrain afferents of VLT integrate thalamo- and tectofugal streams of processing. The tectofugal component is further substantiated by the afferents of the VLT from midbrain SLu, that is know to be a modulatory component of the tectorotundal stream [19].

Our anatomical data reveal a bilateral input from the optic tectum onto VLT. While the ipsilateral afferents also involved input from superficial retinorecipient layers, those from the contralateral side only came from deep laminae that are also involved in bilateral projections onto the rotundus [17]. Tectorotundal neurons can be subdivided into at least five subtypes receiving direct or only indirect retinal input due to their dendritic lamination pattern within or below the termination zone of retinal ganglion cells, respectively [18]. While the majority of cells have direct access to retinal input, one subtype displays dendrites that do not ramify within the retinorecipient layers. Since the dendrites of the ipsi- and the contralateral tectal input to the VLT are likewise confined to the deep layers, they presumably belong to that ascending population which processes indirect visual and/or multimodal information. Accordingly, our stimulation paradigm only revealed very late responses from both eyes. Thus, as outlined above, we suggest that the observed response profile of type I and type II neurons within the VLT result from a bilateral TSM- and TOM-mediated top-down activation of deep tectal layers that subsequently ignite tectal neurons with indirect retinal access.

The projections of VLT provide input to the contralateral VLT (present study) and to tectal layers 11–14 [21] on the ipsilateral side. Thus, VLT neurons not only modulate their counterparts in the contralateral halfbrain but also tectal cells in those layers from which they receive their input (Fig. 5). These deep tectal laminae are in part the source of the diverse descending tectomotor output pathways [20]. Since VLT neurons are partly GABAergic [9], this diencephalic structure could inhibit some tectal circuits while activating others.

4.3. VLT functions in visual processing

The data presented in the present study in conjunction with information from the literature could provide a framework for a tentative interpretation of the function of VLT. First of all, our anatomical results show tectal afferents to VLT to mainly arise from the lateral tectum. Since the lateral tectum represents the central fovea which points into the lateral field of view [34], bilateral visual information within VLT mainly arises from non-overlapping parts of the visual field perceived by the two eyes. Pigeons that fixate stimuli with their left or their right lateral visual field often subsequently make a head or body movement to this target [12]. The descending telencephalotectal projections via TSM and TOM play a key role in mediating this decision to move either to the left or to the right [16]. In both cases, visuomotor systems in both halfbrains have to be coordinated. Accordingly, the physiological properties of both types of VLT cells make a bihemispheric gating function likely. Type I neurons were activated by both left and right eye stimulation, but bilateral stimulation caused a critical time shift in their neuronal responses. Type II neurons completely ignored unilateral stimuli but only responded to the bilateral flash. Thus, the VLT output to deep tectal layers required a bilateral activation of the telencephalo-tecto-VLT system. With their bilateral integration of the tecto- and thalamofugal system and their projections onto the deep tectal layers, VLT neurons could play a role in this bilateral visuomotor control. Obviously, this interpretation of the function of VLT is presently speculative and in need of information on more critical details. However, if it explains at least some functions of this thalamic structure, the bilateral integration at the level of VLT indeed would be part of a system that coordinates visuomotor behavior that is controlled by forebrain circuits of both hemispheres and is executed by tectomotor mechanisms.

Acknowledgements

We thank Burkhard Hellmann for help with the tracer injections and the discussion of the anatomical data. This work was supported by the Deutsche Forschungsgemeinschaft (Sonderforschungsbereich 509: Neurovision).

References

[1] P. Bagnoli, W.K. Francesconi, F. Magni, Visual Wulst influences on the optic tectum of the pigeon, Brain Behav. Evol. 14 (1979) 217–237.

[2] P. Bagnoli, W.K. Francesconi, F. Magni, Interaction of optic tract and visual Wulst impulses on single units of the pigeon's optic tectum, Brain Behav. Evol. 16 (1979) 19–37.

[3] P. Bagnoli, S. Grassi, F. Magni, A direct connection between visual Wulst and tectum opticum in the pigeon (*Columba livia*) demonstrated by horseradish peroxidase, Archives italiennes de biologie 118 (1980) 72–88.

[4] N. Brecha, Some observations on the organization of the avian tectum: afferent nuclei and their tectal projections, Thesis, State University of New York, New York, Stony Brook, 1978.

[5] G. Casini, V. Porciatti, G. Fontanesi, P. Bagnoli, Wulst efferents in the little owl *Athena noctua*: an investigation of projections to the optic tectum, Brain Behav. Evol. 39 (1992) 101–115.

[6] C. Deng, L.J. Rogers, Bilaterally projecting neurons in the two visual pathways of chicks, Brain Res. 794 (1998) 281–290.

[7] C. Deng, L.J. Rogers, Organisation of the tectorotundal and SP/IPS-rotundal projections in the chick, J. Comp. Neurol. 394 (1998) 171–185.

[8] J.L. Dubbeldam, A.M. Den Boer-Visser, R.G. Bout, Organization and efferent connections of the archistriatum of the mallard, *Anas platyrhynchos L.*: an Anterograde and Retrograde Tracing Study, J. Comp. Neurol. 388 (1997) 632–657.

[9] L. Domenici, H.J. Waldvogel, C. Matute, P. Streit, Distribution of GABA-like immunoreactivity in the pigeon brain, Neuroscience 25 (1988) 931–950.

[10] D. Ehrlich, R. Mark, An atlas of the primary visual projections in the brain of the chick *Gallus gallus*, J. Comp. Neurol. 223 (1984) 592–610.

[11] J. Engelage, H.J. Bischof, The organization of the tectofugal pathway in birds: a comparative review, in: H.P. Zeigler, H.J. Bischof (Eds.), Vision, Brain and Behavior in Birds, MIT Press, Cambridge, MA, 1993, pp. 137–158.

[12] M.B. Friedman, How birds use their eyes, in: P. Wright, P.G. Caryl, D.M. Vowles (Eds.), Neural and Endocrine Aspects of Behaviour in Birds, Elsevier, Amsterdam, 1975, pp. 181–204.

[13] K. Folta, B. Diekamp, O. Güntürkün, Asymmetrical modes of visual bottom-up and top-down integration in the thalamic nucleus rotundus of pigeons, J. Neurosci. 24 (2004) 9475–9485.

[14] S.H. Fung, D. Burstein, R.T. Born, In vivo microelectrode track reconstruction using magnetic resonance imaging, J. Neurosci. Methods 80 (1998) 215–224.

[15] J.D. Green, A simple microelectrode for recording from the central nervous system, Nature 182 (1958) 962.

[16] O. Güntürkün, H.H. Hoferichter, Neglect after section of a left telencephalotectal tract in the pigeon, Behav. Brain Res. 18 (1985) 1–9.

[17] B. Hellmann, O. Güntürkün, Visual-field-specific heterogeneity within the tecto-rotundal projection of the pigeon, Eur. J. Neurosci. 11 (1999) 2635–2650.

[18] B. Hellmann, O. Güntürkün, Structural organization of parallel information processing within the tectofugal visual system of the pigeon, J. Comp. Neurol. 429 (2001) 94–112.

[19] B. Hellmann, M. Manns, O. Güntürkün, The nucleus isthmi, pars semilunaris as a key component of the tectofugal visual system in the pigeon, J. Comp. Neurol. 436 (2001) 153–166.

[20] B. Hellmann, O. Güntürkün, M. Manns, The tectal mosaic: organization of the descending tectal projections in comparison to the ascending tectofugal pathway in the pigeon, J. Comp. Neurol. 472 (2004) 395–410.

[21] S.P. Hunt, N. Brecha, The avian optic tectum: a synthesis of anatomy and bio-chemistry, in: H. Vanagas (Ed.), Comparative Neurobiology of the Optic Tectum, Plenum Press, New York, 1984, pp. 619–648.

[22] S.P. Hunt, H. Künzle, Observations on the projections and intrinsic organization of the pigeon optic tectum: an autoradiographic study based on anterograde and retrograde axonal and dendritic flow, J. Comp. Neurol. 170 (1976) 153–172.

[23] S.A. Husband, T. Shimizu, Efferent projections of the ectostriatum in the pigeon (*Columba livia*), J. Comp. Neurol. 406 (1999) 329–345.

[24] O. Inzunza, H. Bravo, Foveal topography in the optic nerve and primary visual centers in Falconiforms, Anat. Rec. 235 (1993) 622–631.

[25] H.J. Karten, W. Hodos, A Stereotaxic Atlas of the Brain of the Pigeon, Johns Hopkins Press, Baltimore, 1967.

[26] C. Keysers, B. Diekamp, O. Güntürkün, Evidence for physiological asymmetries in the intertectal connections of the pigeon (Columba livia) and their potential role in brain lateralization, Brain Res. 852 (2000) 406–413.

[27] H. Kuhlenbeck, The ontogenetic development of the diencephalic centers in a bird's brain (chick) and comparison with the reptilian and mammalian diencephalon, J. Comp. Neurol. 66 (1937) 23–75.

[28] H. Kuhlenbeck, The development and structure of the pretectal cell masses in the chick, J. Comp. Neurol. 71 (1939) 361–389.

[29] N. Leresche, O. Hardy, D. Jassik-Gerschenfeld, Receptive field properties of single cells in the pigeon's optic tectum during cooling of the 'visual Wulst', Brain Res. 267 (1982) 225–236.

[30] D. Miceli, H. Gioanni, J. Repérant, J. Peyrichoux, The avian visual Wulst: I. An anatomical study of afferent and efferent pathways. II. An electrophysiological study of the functional properties of single neurons, in: A.M. Granda, J.H. Maxwell (Eds.), Neural Mechanisms of Behavior in Birds, Plenum Press, New York, 1979, pp. 223–254.

[31] D. Miceli, J. Repérant, J. Villalobos, L. Dionne, Extratelencephalic projections of the avian visual wulst. A quantitative autoradiographic study in the pigeon *Columba livia*, J. Hirnforschung 28 (1987) 45–57.

[32] R.B. Norgren Jr., R. Silver, Retinal projections in quail (*Coturnix coturnix*), Vis. Neurosci. 3 (1989) 377–387.

[33] A. Reiner, D.J. Perkel, L.L. Bruce, A.B. Butler, A. Csillag, W. Kuenzel, L. Medina, G. Paxinos, T. Shimizu, G. Striedter, M. Wild, G.F. Ball, S. Durand, O. Güntürkün, D.W. Lee, C.V. Mello, A. Powers, S.A. White, G. Hough, L. Kubikova, T.V. Smulders, K. Wada, J. Dugas-Ford, S. Husband, K. Yamamoto, J. Yu, C. Siang, E.D. Jarvis, Revised nomenclature for avian telencephalon and some related brainstem nuclei, J. Comp. Neurol. 473 (2004) 377–414.

[34] M. Remy, O. Güntürkün, Retinal afferents of the tectum opticum and the nucleus opticus principalis thalami in the pigeon, J. Comp. Neurol. 305 (1991) 57–70.

[35] H. Rendahl, Embryologische und morphologische Studien über das Zwischenhirn beim Huhn, Acta Zool. 5 (1924) 214–344.

[36] J. Repérant, Nouvelles donnes sur les projections visuelles chez le pigeon (*Columba livia*), J. Hirnforschung 14 (1973) 151–182.

[37] T. Shimizu, H.J. Karten, The avian visual system and the evolution of the neocortex, in: H.P. Zeigler, H.J. Bischof (Eds.), Vision, Brain, and Behavior in Birds, The MIT Press, Cambridge, MA, 1993, pp. 103–114.

[38] T. Shimizu, K. Cox, H.J. Karten, Intratelencephalic projections of the visual Wulst in pigeons (*Columba livia*), J. Comp. Neurol. 359 (1995) 551–572.

[39] P. Streit, M. Stella, M. Cuénod, Transneuronal labelling in the pigeon visual system, Neuroscience 5 (1980) 763–775.

[40] S. Sugita, K. Taniyama, Retinal projections into the diencephalon in the fowl (*Gallus gallus domesticus*), Kaibogaku Zasshi 65 (1990) 420–435.

[41] M.P. Theiss, B. Hellmann, O. Güntürkün, The architecture of an inhibitory sidepath within the avian tectofugal system, Neuroreport 14 (2003) 879–882.

[42] J. Voss, H.J. Bischof, Regulation of ipsilateral visual information within the tectofugal visual system in zebra finches, J. Comp. Physiol. A 189 (2003) 545–553.

[43] C.C. Wu, H.J. Karten, The thalamo-hyperstriatal system is established by the time of hatching in chicks (*Gallus gallus*): a cholera toxin B subunit study, Vis. Neurosci. 15 (1998) 349–358.

[44] J. Yano, The EEG response to repetitive photic stimulation in various regions of the chicken brain, Electroencephalogr. Clin. Neurophysiol. 40 (1976) 244–252.